

# Tracking and Sampling of a Phytoplankton Patch by an Autonomous Underwater Vehicle in Drifting Mode

Yanwu Zhang, Brian Kieft, Robert McEwen, Jordan Stanway, James Bellingham, John Ryan, Brett Hobson, Douglas Pargett, James Birch, and Christopher Scholin

**Abstract**—Phytoplankton patches in the coastal ocean have important impacts on the patterns of primary productivity, the survival and growth of zooplankton and fish larvae, and the development of harmful algal blooms (HABs). We desire to observe microscopic life in a phytoplankton patch in its natural frame of reference (which is moving with the ocean current), thereby permitting resolution of time-dependent evolution of the population. To achieve this goal, we have developed a method for a Tethys-class long range autonomous underwater vehicle (AUV) (which has a propeller and a buoyancy engine) to detect, track, and sample a phytoplankton patch in buoyancy-controlled drifting mode. In this mode, the vehicle shuts off its propeller and actively controls its buoyancy to autonomously find the peak-chlorophyll layer, stay in it, and trigger water sampling in the layer. In an experiment in Monterey Bay, CA in July 2015, the Makai AUV, which was equipped with a prototype 3rd-generation Environmental Sample Processor (3G-ESP), ran the algorithm to autonomously detect the peak-chlorophyll layer, and drifted and triggered ESP samplings in the layer.

**Index Terms**—Autonomous underwater vehicle (AUV), Environmental Sample Processor (ESP), phytoplankton patch, peak detection, drifting, tracking, sampling.

## I. INTRODUCTION

Phytoplankton patches in the coastal ocean have important impacts on the patterns of primary productivity, the survival and growth of zooplankton and fish larvae, and the development of harmful algal blooms (HABs) [1]–[5]. We desire to observe microscopic life in a phytoplankton patch in its natural frame of reference (which is moving with the ocean current), thereby permitting resolution of time-dependent evolution of the population [6]–[8]. Toward this end, we have developed a method for a Tethys-class long-range autonomous underwater vehicle (AUV) (which has a propeller and a buoyancy engine) [9], [10] to detect, track, and sample a phytoplankton patch in buoyancy-controlled drifting mode.

A Tethys-class long-range AUV [9] is a propeller-driven vehicle that can run at a speed between 0.5 to 1 m/s. It has a length of 2.3 m  $\sim$  3.2 m (depending on payload configuration), and a diameter of 0.3 m at the midsection.

Y. Zhang, B. Kieft, R. McEwen, J. Stanway, J. Ryan, B. Hobson, D. Pargett, J. Birch, and C. Scholin are with the Monterey Bay Aquarium Research Institute, 7700 Sandholdt Road, Moss Landing, CA 95039. J. Bellingham is currently with the Woods Hole Oceanographic Institution, Woods Hole, MA 02543. Email of the corresponding author Yanwu Zhang: yzhang@mbari.org

The AUV also has an oil-filled buoyancy engine which enables the vehicle to drift at neutral buoyancy at lower power consumption [10]. The AUV thus combines the capabilities of propeller-driven and buoyancy-driven vehicles. The AUV's sensor suite includes Neil Brown temperature and conductivity sensors, a Keller depth sensor, a WET Labs ECO-Triplet Puck fluorescence/backscatter sensor, an Aanderaa dissolved oxygen sensor, an In Situ Ultraviolet Spectrophotometer (ISUS) nitrate sensor, a LI-COR Photosynthetically Active Radiation (PAR) sensor, and a LinkQuest or Rowe Doppler velocity log (DVL).

The AUV's buoyancy engine comprises an internal oil reservoir, an external oil bladder, and a pumping system that moves the oil between the internal reservoir and the external bladder to adjust the vehicle's buoyancy. The buoyancy adjustment principle is the same as that for floats [11] and gliders [12], [13]. However, we use a gear pump that can move oil in both directions which allows for fast and accurate buoyancy adjustment. The oil volume in the internal reservoir is measured using a string potentiometer connected to the piston, based on which the oil volume in the external bladder is deduced for calculating the buoyancy. To decrease buoyancy, the buoyancy control system moves oil from the external bladder to the internal reservoir. Conversely, to increase buoyancy, the system moves oil in the opposite direction. Prior to a science deployment, the AUV runs ballast tests (in a test tank and then in the ocean) to determine the proper oil volume (in the external bladder) for achieving neutral buoyancy.

The Environmental Sample Processor (ESP) is a submersible robotic instrument that performs real-time, autonomous sample acquisition and in-situ molecular analysis using DNA and protein probe arrays, to identify microorganisms as well as as phycotoxins [14], [15]. To enable mobile ecogenomic sensing, a compact and modular 3rd-generation ESP (3G-ESP) is developed and installed in the Makai long range AUV [16]. The 3.2 m long, 160 kg Makai AUV is shown in Figure 1. This integration combines the ESP's autonomous sampling and genomic sensing capabilities and the long range AUV's mobility, persistence, multidisciplinary sensor suite, and targeted sampling capabilities. In the 3G-ESP, each water sampling unit is contained in a cartridge, installed on a circular wheel [16]. Up to 60 cartridges can be installed. Seawater ports connecting to a center ring of valves provide each cartridge access to the seawater supply. The water samples can be

preserved for later analysis in the laboratory, or processed immediately for real-time reporting.

To efficiently and intelligently use this system, we develop targeted sampling algorithms for the AUV to autonomously find the targeted oceanographic feature and trigger ESP sampling in the feature. In this paper, we present a method and experimental results of using the ESP-bearing AUV to detect, track, :



Fig. 1. The Makai long range AUV which is equipped with a 3G-ESP.

## II. AUTONOMOUS DETECTION, TRACKING, AND SAMPLING OF THE PEAK-CHLOROPHYLL LAYER IN DRIFTING MODE

We previously developed peak-capture methods for an AUV in flight mode (on a sawtooth trajectory in the vertical dimension) to accurately detect and trigger water sampling in a phytoplankton thin layer [17] or subsurface oil plume [18]. Based on this method, we designed the drifting-mode autonomous peak detection and tracking algorithm which comprises the following key components.

### A. Low-Pass Filtering of Chlorophyll Measurement

To remove spurious peaks due to measurement noise, the raw chlorophyll measurement is low-pass filtered by an  $N$ -sample moving-average window:

$$Chl_{lp}(n) = \frac{1}{N} \sum_{i=0}^{N-1} Chl(n-i) \quad (1)$$

where  $n$  is the index of the current time;  $Chl(n)$  is the raw chlorophyll measurement;  $Chl_{lp}(n)$  is the low-pass filtered signal. Note that this low-pass filter leads to a delay of  $\frac{(N-1)}{2}$  samples.

### B. Detection of the Peak-Chlorophyll Layer, and Drifting and Sampling in the Layer

Suppose a peak chlorophyll layer lies somewhere between the sea surface and a certain depth bound  $Dep_{DeepBound}$ . The AUV operates in the following steps to autonomously find the peak chlorophyll layer, and drift and sample in the layer, as illustrated in Figure 2.

- 1) The AUV shuts off its propeller. From the surface, the vehicle decreases buoyancy to descend to  $Dep_{DeepBound}$ . On the descent, the AUV seeks

$Chl_{lp\_max}$  (the peak of the  $Chl_{lp}$  signal) and the corresponding depth  $DEP_{ChlPeak}$ .

- 2) When reaching depth  $Dep_{DeepBound}$ , the vehicle increases buoyancy to turn to an ascent. To confirm the turn from descent to ascent, the AUV checks the following two conditions [19]: 1) The depth has decreased four times in a row. 2) The depth has decreased from the maximum depth by more than 1 m. Once the turn is confirmed, the vehicle reports the peak signal value  $Chl_{lp\_max}$  of the entire descent leg and the corresponding depth  $DEP_{ChlPeak}$ . In the mission script, the value of  $DEP_{ChlPeak}$  is saved at depth  $Dep_{DeepBound} - 1.5$  m on the ascent leg.
- 3) On the ascent, when the AUV reaches depth  $DEP_{ChlPeak}$ , it controls buoyancy to stop and remain at that depth. It takes a few minutes for the initial depth overshoot to damp down. Then the AUV can trigger water sampling at pre-programmed time intervals or on an adaptive sampling scheme (i.e., when certain water-property conditions are met).

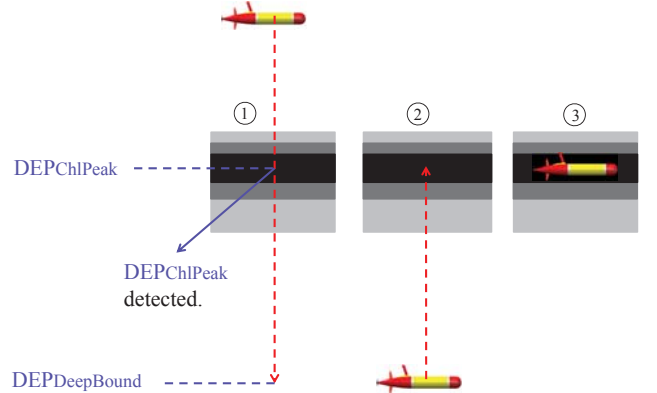


Fig. 2. Illustration of the algorithm for autonomous detection of the peak-chlorophyll layer, and drifting and sampling in the layer. The darkness level represents the chlorophyll signal level — the darker, the higher chlorophyll signal level. The darkest layer represents the peak-chlorophyll layer.

### C. Reacquiring the Peak-Chlorophyll Layer When It Moves up or Down

Phytoplankton patches move over time due to environmental conditions and phytoplankton's behavior. For example, diurnal vertical migration of phytoplankton [20] will cause a peak chlorophyll layer to move up or down. While the AUV drifts at depth  $DEP_{ChlPeak}$ , it keeps monitoring the chlorophyll signal level. Vertical displacement of the peak chlorophyll layer will cause the AUV-measured chlorophyll signal level at  $DEP_{ChlPeak}$  (the old peak depth) to drop.

When the chlorophyll signal level drops below a certain threshold, the AUV will restart a vertical search to find the new peak-chlorophyll depth and track the layer. Presuming the new peak-chlorophyll depth  $DEP_{ChlPeak\_new}$  lies within a vertical distance of  $VertPerburb$  from  $DEP_{ChlPeak}$  (i.e., within a depth range  $DEP_{ChlPeak} \pm VertPerburb$ ), the peak reacquisition steps are as follows, as illustrated in Figure 3.

- 1) When  $Chl_{lp}$  (monitored by the AUV) falls below  $Chl_{lp\_max} \times \alpha$  where  $\alpha$  is a fraction value smaller than one (e.g., 0.7), the AUV determines that the peak layer has moved up or down, away from the tracked depth. The vehicle increases buoyancy to ascend to depth  $DEP_{ChlPeak} - VertPerburb$ .
- 2) When reaching depth  $DEP_{ChlPeak} - VertPerburb$ , the AUV decreases buoyancy to descend to depth  $DEP_{ChlPeak} + VertPerburb$ . On the descent, the vehicle seeks  $Chl_{lp\_max\_new}$  (the new peak of the  $Chl_{lp}$  signal) and the corresponding depth  $DEP_{ChlPeak\_new}$ .
- 3) When reaching depth  $DEP_{ChlPeak} + VertPerburb$ , the vehicle increases buoyancy to turn to an ascent. Once the turn is confirmed, the vehicle reports the peak signal value  $Chl_{lp\_max\_new}$  of the preceding descent leg and the corresponding depth  $DEP_{ChlPeak\_new}$ . In the mission script, the value of  $DEP_{ChlPeak\_new}$  is saved at depth  $DEP_{ChlPeak} + VertPerburb - 1.5$  m on the ascent leg.
- 4) On the ascent, when the AUV reaches depth  $DEP_{ChlPeak\_new}$ , it controls buoyancy to stop and remain at that depth. After the initial depth overshoot damps down, the AUV can trigger water sampling when drifting at  $DEP_{ChlPeak\_new}$ .

However, within each water sampling duration, the AUV will maintain its depth to guarantee consistency of the water sample.

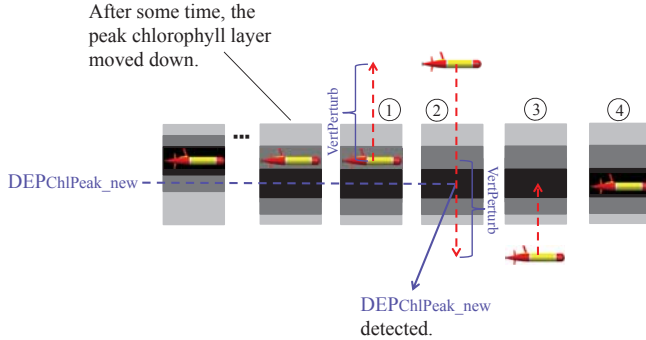


Fig. 3. Illustration of the algorithm for reacquiring the peak-chlorophyll layer when it moves down. The darkness level represents the chlorophyll signal level as in Figure 2.

### III. FIELD EXPERIMENT

In July 2015, we tested a prototype 3G-ESP (containing 5 water sampling cartridges) on the Makai long range AUV in Monterey Bay, CA. The AUV ran the presented algorithm to autonomously detect the peak-chlorophyll layer, and triggered ESP samplings in the layer (and away from the layer for comparisons). The five water samples were acquired in two AUV missions described as follows.

#### A. The First AUV Mission

In the first mission on 22 July 2015, the Makai AUV started with an initial yo-yo survey (as shown in the left part of Figure 4), through which a subsurface chlorophyll layer was observed. After a quick inspection of the transmitted data that showed this layer, the shore operator issued a command to the AUV to start the autonomous peak detection and sampling mission, as shown in the right part of Figure 4. The AUV's depth and chlorophyll measurements are shown in Figure 5. The vehicle was in drifting mode (with the propeller shut off) in the peak-detection phase and in the break between the two ESP sampling durations, but in each sampling duration the vehicle turned on the propeller to run circles at the peak-chlorophyll depth. Hence each water sample is a mixture of water taken over some horizontal scale.

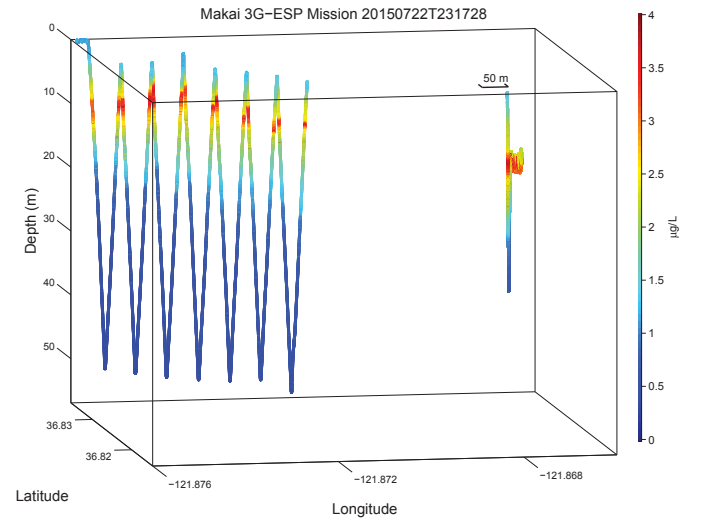


Fig. 4. The Makai AUV's initial yo-yo survey (left part), followed by the autonomous peak detection and sampling mission (right part).

With the propeller shut off, the vehicle decreased buoyancy to descend from the surface.  $Dep_{DeepBound}$  was set to 30 m, given the prior information that the chlorophyll layer was shallower than this depth. On this descent, the AUV detected the chlorophyll peak at  $DEP_{ChlPeak} = 10.6$  m and the peak signal level was  $Chl_{lp\_max} = 3.6 \mu\text{g/L}$ .

The sampling frequency of the raw chlorophyll fluorescence measurement was 10 Hz (i.e., 0.1 s sampling interval). We set the low-pass filter window length  $N = 20$  (equivalent to 2 s) to suppress measurement noise. This low-pass filter leads to a delay of  $\frac{(N-1)}{2} \approx 10$  samples, equivalent to 1 s time delay. The AUV's descent speed was about 0.04 m/s. Therefore, the 1 s time delay corresponded to a 0.04 m error in the reported peak-chlorophyll depth. Considering phytoplankton thin layers' typical thickness of tens of centimeters to a few meters, this depth error is negligible. Nevertheless, to guarantee accuracy when a longer low-pass filter is used, we will correct this error in the improved program, as done in a previously developed flight-mode AUV peak-capture algorithm [18].

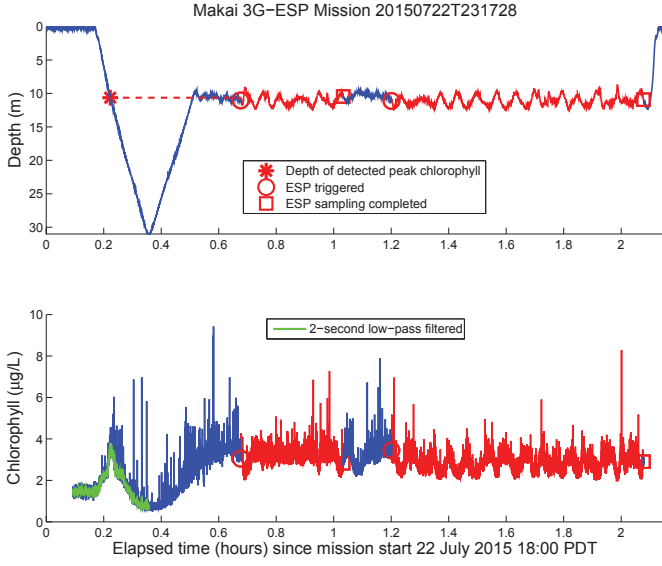


Fig. 5. The AUV's depth and chlorophyll measurements during the first peak detection and sampling mission. The low-pass filtered chlorophyll signal  $Chl_{lp}$  is shown in green in the lower panel. The peak-chlorophyll detection point is marked by the asterisk in the upper panel. The starting and ending points of the two ESP samplings are marked in both panels.

When reaching 30 m depth, the AUV increased buoyancy to turn to an ascent. When reaching the peak-chlorophyll depth, the vehicle controlled buoyancy to stop and remain at that depth. After a 10-minute interval for the depth overshoot to damp down, the AUV turned on the propeller to 300 RPM (corresponding to 1 m/s speed) and set the rudder angle to  $13^\circ$  to run in circles at the peak-chlorophyll depth. The AUV triggered ESP sample #1 at 11.0 m depth. The sampling process took about 21 minutes. Then the AUV turned off the propeller and reset the rudder angle to zero. After a 10-minute interval, the AUV again turned on the propeller to 300 RPM and set the rudder angle to  $13^\circ$  to resume circling at the peak-chlorophyll depth. The AUV triggered ESP sample #2 at 11.0 m depth. The sampling process took about 53 minutes. Once the sampling was completed, the mission terminated and the vehicle ascended to the surface.

### B. The second AUV Mission

In the second mission on 24 July 2015, the Makai AUV also started with an initial yo-yo survey (as shown in the left part of Figure 6), through which a subsurface chlorophyll layer was observed. The shore operator issued a command to the AUV to start the autonomous peak detection and sampling mission, as shown in the right part of Figure 6. The AUV's depth and chlorophyll measurements are shown in Figure 7. Throughout this mission, the vehicle was in drifting mode, with the propeller shut off and the rudder angle set to zero.

The AUV decreased buoyancy to descend from the surface to  $Dep_{DeepBound} = 30$  m. On this descent, the AUV detected the chlorophyll peak at  $DEP_{ChlPeak} = 13.4$  m and the peak signal level was  $Chl_{lp,max} = 4.9$   $\mu\text{g/L}$ .

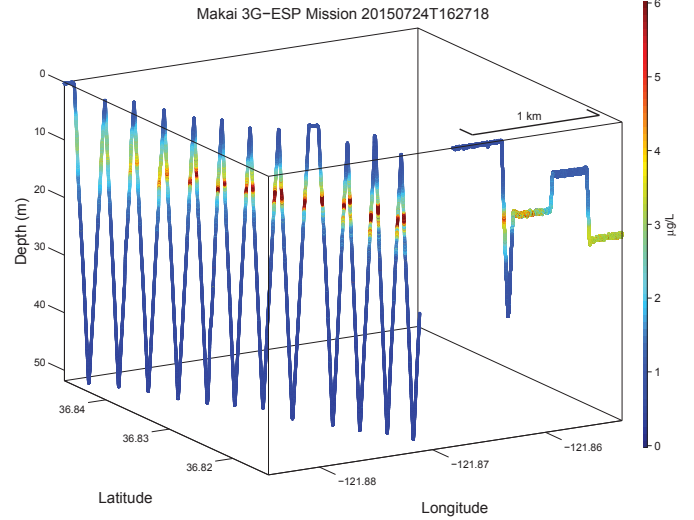


Fig. 6. The Makai AUV's initial yo-yo survey (left part), followed by the second autonomous peak detection and sampling mission (right part).

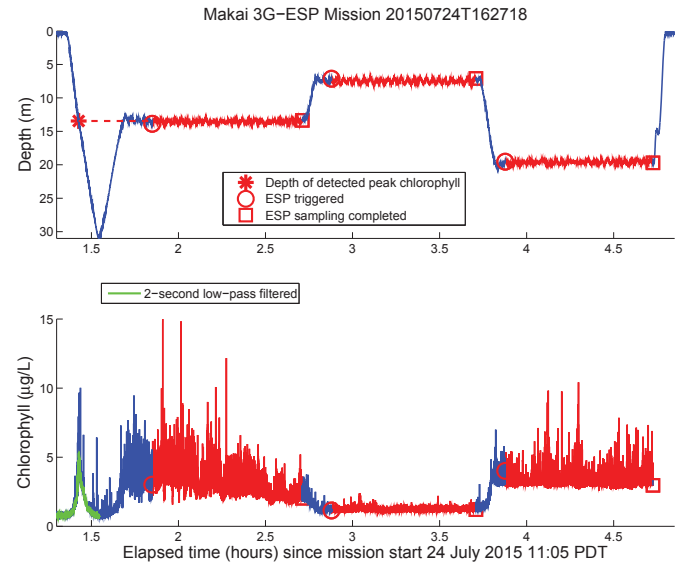


Fig. 7. The AUV's depth and chlorophyll measurements during the second peak detection and sampling mission.

When reaching 30 m depth, the AUV increased buoyancy to turn to an ascent. When reaching the peak-chlorophyll depth, the vehicle controlled buoyancy to stop and remain at that depth. After a 10-minute interval for the depth overshoot to damp down, the AUV triggered ESP sample #3 at 13.8 m depth. The sampling process took about 51 minutes. The depth undulation range during the sampling process was [13.0 m 14.0 m], within  $\pm 0.6$  m from  $DEP_{ChlPeak} = 13.4$  m.

Subsequently the AUV moved up to 6 meters above  $DEP_{ChlPeak}$ , and after a 10-minute interval, triggered ESP sample #4 (the sampling process took about 50 minutes). Then the vehicle moved down to 6 meters below  $DEP_{ChlPeak}$ ,

and after a 10-minute interval, triggered ESP sample #5 (the sampling process took about 50 minutes). These two samples are for comparison with the “in-layer” sample #3.

Note that over the 3-hour drifting and sampling process, the vehicle drifted eastward for about 0.85 km. The current speed was estimated to be about 0.08 m/s.

#### IV. CONCLUSION

We have developed a method for a Tethys-class long range AUV to autonomously detect, track, and sample a phytoplankton patch in buoyancy-controlled drifting mode. In an experiment in Monterey Bay in July 2015, an ESP-bearing long range AUV demonstrated the method by autonomously detecting the peak-chlorophyll layer, and acquiring five water samples in the layer (and away from the layer for comparison). The water samples are being analyzed. On the basis of this algorithm, we will design methods to enable multi-AUV collaborative tracking and sampling of chlorophyll patches.

#### ACKNOWLEDGMENT

This work was supported by the David and Lucile Packard Foundation. The authors thank William Ussler and Ed Mellinger for helping with the Makai AUV operations. The authors thank Brent Roman and Carlos Rueda for the work on programming and testing the AUV-ESP software interface. The authors are also thankful to Jon Erickson for providing materials about the AUV’s buoyancy engine design, and to Christina Preston for analyzing the ESP water samples.

#### REFERENCES

- [1] T. J. Cowles, R. A. Desiderio, and M.-E. Carr, “Small-scale planktonic structure: Persistence and trophic consequences,” *Oceanography*, vol. 11, no. 1, pp. 4–9, 1998.
- [2] J. M. Sullivan, M. A. McManus, O. M. Cheriton, K. J. Benoit-Bird, L. Goodman, Z. Wang, J. P. Ryan, M. Stacey, D. V. Holliday, C. Greenlaw, M. A. Moline, and M. McFarland, “Layered organization in the coastal ocean: an introduction to planktonic thin layers and the LOCO project,” *Continental Shelf Research*, vol. 30, no. 1, pp. 1–6, 2010.
- [3] M. A. McManus, R. M. Kudela, M. W. Silver, G. F. Steward, P. L. Donaghay, and J. M. Sullivan, “Cryptic blooms: Are thin layers the missing connection?” *Estuaries and Coasts: J CERF*, vol. 31, pp. 396–401, 2008.
- [4] J. P. Ryan, M. A. McManus, J. D. Paduan, and F. P. Chavez, “Phytoplankton thin layers caused by shear in frontal zones of a coastal upwelling system,” *Marine Ecology Progress Series*, vol. 354, pp. 21–34, 2008.
- [5] J. P. Ryan, M. A. McManus, and J. M. Sullivan, “Interacting physical, chemical and biological forcing of phytoplankton thin-layer variability in Monterey Bay, California,” *Continental Shelf Research*, vol. 30, no. 1, pp. 7–16, 2010.
- [6] MBARI, “A new view of microbial life near the sea surface,” *Monterey Bay Aquarium Research Institute Annual Report*, pp. 26–29, 2011.
- [7] J. C. Robidart, M. J. Church, J. P. Ryan, F. Ascani, S. T. Wilson, D. Bombar, R. M. III, K. J. Richards, D. M. Karl, C. A. Scholin, and J. P. Zehr, “Ecogenomic sensor reveals controls on N<sub>2</sub>-fixing microorganisms in the North Pacific ocean,” *The ISME Journal*, vol. 8, pp. 1175–1185, 2014.
- [8] E. A. Ottesen, C. R. Young, S. M. Gifford, J. M. Eppley, R. M. III, S. C. Schuster, C. A. Scholin, and E. F. DeLong, “Multispecies diel transcriptional oscillations in open ocean heterotrophic bacterial assemblages,” *Science*, vol. 345, no. 6193, pp. 207–212, 2014.
- [9] J. G. Bellingham, Y. Zhang, J. E. Kerwin, J. Erikson, B. Hobson, B. Kieft, M. Godin, R. McEwen, T. Hoover, J. Paul, A. Hamilton, J. Franklin, and A. Banka, “Efficient propulsion for the Tethys long-range autonomous underwater vehicle,” *IEEE AUV 2010*, pp. 1–6, Monterey, CA, September 2010.
- [10] B. Hobson, J. G. Bellingham, B. Kieft, R. McEwen, M. Godin, and Y. Zhang, “Tethys-class long range AUVs - extending the endurance of propeller-driven cruising AUVs from days to weeks,” *Proc. IEEE AUV 2012*, pp. 1–8, Southampton, U.K., September 2012.
- [11] R. E. Davis, D. C. Webb, L. A. Regier, and J. Dufour, “The autonomous lagrangian circulation explorer (ALACE),” *Journal of Atmospheric and Oceanic Technology*, vol. 9, pp. 264–285, 1992.
- [12] C. C. Eriksen, T. J. Osse, R. D. Light, T. Wen, T. W. Lehman, P. L. Sabin, J. W. Ballard, and A. M. Chiodi, “Seaglider: a long-range autonomous underwater vehicle for oceanographic research,” *IEEE Journal of Oceanic Engineering*, vol. 26, no. 4, pp. 424–436, October 2001.
- [13] J. Sherman, R. E. Davis, W. B. Owens, and J. Valdes, “The autonomous underwater glider “Spray”,” *IEEE Journal of Oceanic Engineering*, vol. 26, no. 4, pp. 437–446, October 2001.
- [14] C. Scholin, G. Doucette, S. Jensen, B. Roman, D. Pargett, R. M. III, C. Preston, W. Jones, J. Feldman, C. Everlove, A. Harris, N. Alvarado, E. Massion, J. Birch, D. Greenfield, R. Vrijenhoek, C. Mikulski, and K. Jones, “Remote detection of marine microbes, small invertebrates, harmful algae and biotoxins using the Environmental Sample Processor (ESP),” *Oceanography*, vol. 22, pp. 158–167, 2009.
- [15] C. A. Scholin, *Ecogenomic sensors. In Encyclopedia of Biodiversity, Volume 2 (Levin S. A. (ed.))*, 2nd ed. Waltham, MA: Academic Press, pp. 690–700, 2013.
- [16] D. M. Pargett, J. M. Birch, C. M. Preston, J. P. Ryan, Y. Zhang, and C. A. Scholin, “Development of a mobile ecogenomic sensor,” *Proc. MTS/IEEE Oceans ’15*, pp. 1–6, Washington, D.C., October 2015.
- [17] Y. Zhang, R. S. McEwen, J. P. Ryan, and J. G. Bellingham, “Design and tests of an adaptive triggering method for capturing peak samples in a thin phytoplankton layer by an autonomous underwater vehicle,” *IEEE Journal of Oceanic Engineering*, vol. 35, no. 4, pp. 785–796, October 2010.
- [18] Y. Zhang, R. S. McEwen, J. P. Ryan, J. G. Bellingham, H. Thomas, C. H. Thompson, and E. Rienecker, “A peak-capture algorithm used on an autonomous underwater vehicle in the 2010 Gulf of Mexico oil spill response scientific survey,” *Journal of Field Robotics*, vol. 28, no. 4, pp. 484–496, July/August 2011.
- [19] Y. Zhang, J. G. Bellingham, M. A. Godin, and J. P. Ryan, “Using an autonomous underwater vehicle to track the thermocline based on peak-gradient detection,” *IEEE Journal of Oceanic Engineering*, vol. 37, no. 3, pp. 544–553, July 2012.
- [20] J. M. Sullivan, P. L. Donaghay, and J. E. B. Rines, “Coastal thin layer dynamics: Consequences to biology and optics,” *Continental Shelf Research*, vol. 30, no. 1, pp. 50–65, 2010.